Multi-station probing of thunderstorm-generated D-layer fluctuations by using time-domain lightning waveforms

E. H. Lay[1] and X.-M. Shao[1]

Received 23 September 2011; revised 4 November 2011; accepted 7 November 2011; published 13 December 2011.

[1] This study uses multi-station time-domain very-low and low-frequency (VLF/LF) lightning waveforms detected from a range of several hundred kilometers to probe fluctuations in D-layer ionospheric height and peak reflection ratio in three regions near a large thunderstorm on the night of 17 June 2005. These measurements show propagation of the fluctuations away from the thunderstorm in addition to a background eastward-propagating fluctuation over the entire region. Measured speeds of propagation range from ∼45 m/s to ∼85 m/s, consistent with horizontal propagation speeds of atmospheric gravity waves. The fluctuation propagation is seen in both the ionospheric height measurement and the peak reflection ratio measurement with similar periods and speeds. Ionospheric height perturbations in the measured regions can be as large as 6 km from average, and perturbations in peak reflection ratio can be as large at 100%. **Citation:** Lay, E. H., and X.-M. Shao (2011), Multi-station probing of thunderstorm-generated D-layer fluctuations by using time-domain lightning waveforms, *Geophys. Res. Lett.*, *38*, L23806, doi:10.1029/2011GL049790.

1. Introduction

[2] The D-layer ionosphere has been studied for decades by measuring the amplitude and phase of narrowband very-low frequency (VLF; 3–30 kHz) transmitters and inferring the electron density profile from the measurements [i.e., *Wait and Spies*, 1964; *Bickel et al.*, 1970; *Pappert and Ferguson*, 1986, and references therein]. These measurements probe the average behavior of the D-layer over very long great-circle paths, especially in the daytime [i.e., *McRae and Thomson*, 2000; *Thomson et al.*, 2005]. They also have been used to study D-layer heating due to thunderstorm quasi-electrostatic fields [*Inan et al.*, 1996; *Pasko et al.*, 1995]. Recently, a technique has used VLF radiation from lightning sferics to probe the D-layer [i.e., *Cummer et al.*, 1998; *Cheng et al.*, 2007; *Han and Cummer*, 2010]. The aforementioned studies all make path-averaged measurements of the D-layer by using frequency-domain mode-propagation techniques.

[3] Recent work that was motivated by the studies of *Shao and Jacobson* [2009] and *Jacobson et al.* [2009] has presented a new method of probing the D-layer ionosphere by analysis of time-domain cloud-to-ground lightning waveforms [*Lay and Shao*, 2011]. This technique allows high temporal and spatial resolution measurements of ionospheric fluctuations in height and reflectivity by using first-hop ionospheric reflections of the lightning signal in the time-domain instead of frequency-domain mode propagation. Initial analysis making use of this technique suggested significant fluctuation in the nighttime ionosphere near a thunderstorm on spatial scales of tens of kilometers and over time periods of hours [*Lay and Shao*, 2011]. The fluctuation periods, possible propagation speed, and inferred propagation direction are consistent with recent observations and model studies of atmospheric gravity waves (AGW) at the D-layer altitude that are originated from convective thunderstorm activity overshooting the tropopause [*Alexander et al.*, 1995; *Vadas and Fritts*, 2004; *Vadas et al.*, 2009; *Yue et al.*, 2009].

[4] However, the results presented by *Lay and Shao* [2011] only show measurements of perturbations in a single region north of a thunderstorm. In this paper, the same technique is used for data analysis, but perturbations from several locations surrounding a storm are analyzed to better determine the direction of propagation of the fluctuations.

2. Data Analysis

[5] All measurements in this paper are from the Los Alamos Sferic Array (LASA), which detects lightning in the 0.2–500 kHz frequency range [*Shao et al.*, 2006]. Data analyzed for this report were detected on 17 June 2005 between 0400 UT and 0800 UT (2300 to 0300 local time). The location of the lightning during this period is shown in Figure 1 as colored dots, with the color indicating the time of the lightning. Although the study is focused on the nighttime D-layer, lightning activity is shown starting from 0000 UT (1900 LT) instead of 0400 UT since thunderstorm activity from an earlier time could be the cause of ionospheric perturbations later. The lightning time waveforms detected at three LASA stations (marked as LNK, LAM, and LBB in Figure 1) are used in this paper to determine fluctuations in the ionosphere midway between the storm and the respective stations. The approximate ionospheric regions probed by the LNK, LAM, and LBB stations are shaded gray in Figure 1. The GCK and OUN stations are not analyzed in this paper because the majority of the lightning strokes are less than 350 km away from the two stations, making it difficult to accurately select the ionospheric reflection from the waveform. Measurements from the GRL station are not presented because the measured region lies above another storm cell that is just to the northwest of the GCK station (Figure 1). In this case, it would be difficult to separate out the AGW effects due to the main storm of interest from possible perturbations associated with electrostatic or electromagnetic effects due to the storm cell directly below the probed region.

[6] The VLF/LF signal from each lightning stroke propagates to the receiving stations at distances of 350 to 1000 km as a direct ground wave followed by a delayed ionospheric reflection. The time delay and magnitude of the ionospheric reflection vary as the D-layer height and electron density is modified. Each signal can be received at 6 LASA stations,

[1]Space and Remote Sensing Group, Los Alamos National Laboratory, Los Alamos, New Mexico, USA.

Copyright 2011 by the American Geophysical Union.
0094-8276/11/2011GL049790

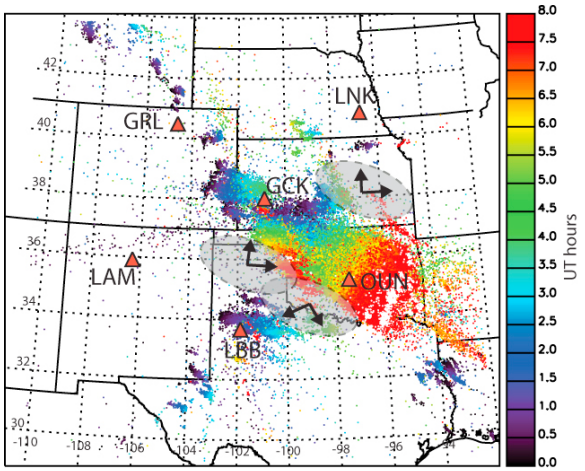

Figure 1. The 100,000+ negative cloud-to-ground lightning strokes on 17 June 2005 color-coded by time, with LASA receiving station locations shown as red triangles. Approximate ionospheric regions probed by LNK, LAM, and LBB shown as shaded ovals. Measured azimuthal and radial propagation directions are shown by the arrows.

meaning that each lightning stroke can be used to probe the ionosphere in up to 6 locations (midway between the lightning and each station). For this study, the waveforms from the individual stations are band-pass filtered to 60–120 kHz, the same as the high band in [*Lay and Shao*, 2011]. (Note that the frequency bands were mistakenly documented in [*Lay and Shao*, 2011] by a factor of 2 and were actually 0–60 kHz for low band and 60–120 kHz for high band.) The time delay between the ground wave and the first-hop ionospheric reflection is measured, and an apparent ionospheric height (h) is determined from this time delay by using simple spherical geometry and assuming speed-of-light propagation. In addition, the peak reflection ratio (R) is measured by the magnitude of electric field of the ionospheric reflection over the magnitude of the electric field of the ground wave [*Lay and Shao*, 2011]. This ratio differs

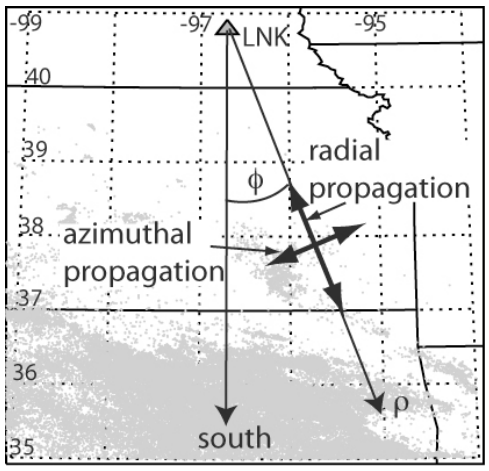

Figure 2. Schematic showing that each measurement location is defined by a range, ρ, and an azimuthal angle, ϕ. Fluctuation propagations can then be measured in two orthogonal directions (radial and azimuthal), shown by double-sided arrows.

from a normally defined ionospheric reflectivity that compares the reflected signal against the incident signal at the lower ionospheric boundary. Instead, R is a measure of the E-field peak ratio between the reflected and ground wave at the sensor location. The measurements h and R depend on lightning-to-station distance because of the non-specular nature of the ionospheric reflection boundary. The average dependence is removed by using the method described by *Lay and Shao* [2011], which results in the quantities of Δh and ΔR for the perturbations in height and peak reflection ratio.

[7] With lightning strokes covering a large spatial spread, the measurements can be used to probe ionospheric features in two-dimensions - radial and azimuthal - as illustrated by the double-sided arrows in Figure 2. As is discussed by *Lay and Shao* [2011], the azimuthal measurement has finer resolution than the radial measurement due to the size of the Fresnel zone in each direction (~35 km radius Fresnel zone for 30 Hz at 500 km azimuthally versus ~110 km radially). For that reason, the azimuthal measurement is able to detect the velocity of the perturbations more clearly than the radial measurement. Nevertheless, the radial measurement can help determine the direction of propagation even though the resolution may not be high enough to determine a speed.

3. Results

[8] Figure 3 presents ionospheric height fluctuations (Δh) versus time as measured by LNK (Figure 3, top), LBB (Figure 3, middle), and LAM (Figure 3, bottom) stations. Radial measurements are presented in the left column, and

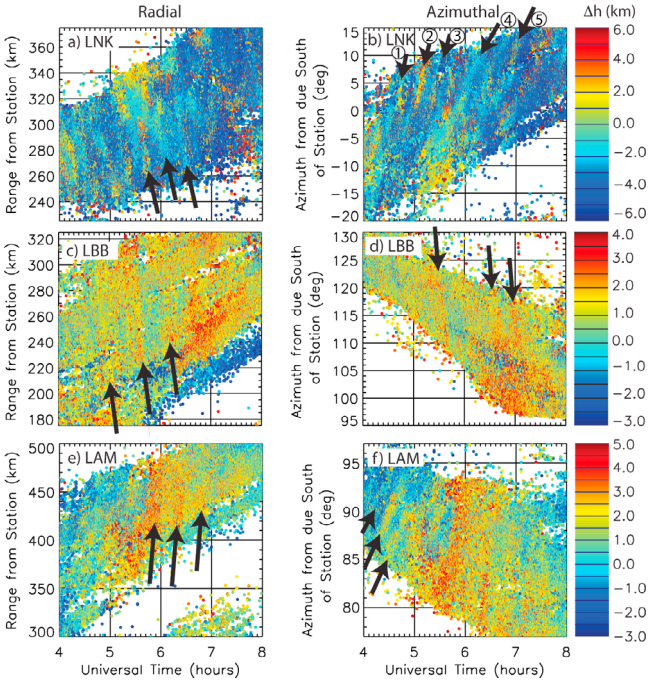

Figure 3. Ionospheric height fluctuations versus time as measured by (a, b) LNK, (c, d) LBB, and (e, f) LAM. Left column shows fluctuations plotted by range from the station, and right column shows them plotted by azimuthal angle. Color indicates change in height from average. Arrows indicate examples of propagating bright features.

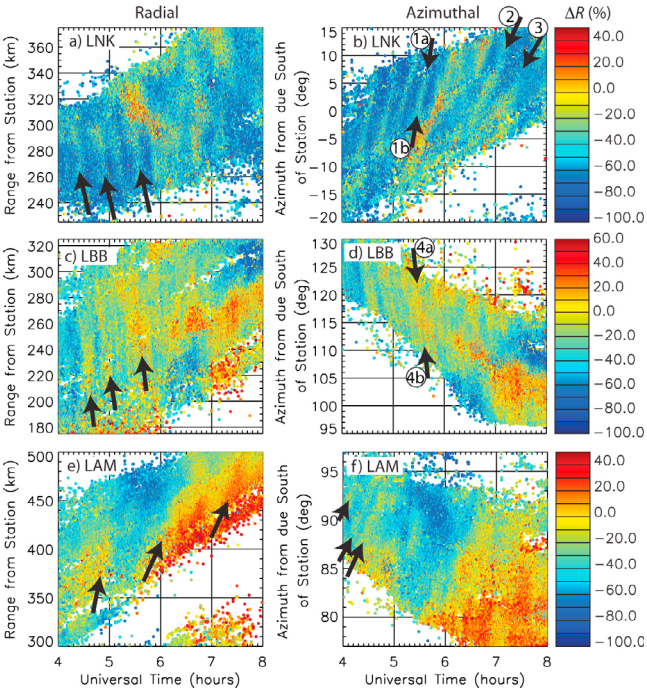

Figure 4. Fluctuations in peak reflection ratio versus time. Same format as Figure 3.

azimuthal measurements are presented in the right column. The color represents the magnitude of the change in the height from average. Figure 4 presents fluctuations in the peak ratio (ΔR, in %) in the same format. The term 'features' is used in this paper to describe a region in which the measurement was consistently above average (bright feature) or consistently below average (dark feature). Arrows overlaid on Figures 3 and 4 indicate examples of several bright features. Features that are sloped in the range-vs-time plots (Figures 3a, 3c, 3e, 4a, 4c, and 4e) propagate in the radial direction (illustrated in Figure 2). Features sloped in the azimuth-vs-time plots (Figures 3b, 3d, 3f, 4b, 4d, and 4f) propagate in the azimuthal direction (Figure 2). Stationary features have no slope in Figures 3 and 4.

[9] The azimuthal plots for LNK (Figures 3b and 4b) show features with clear propagation from smaller angles to larger angles over time (positive slope), indicating an eastward propagation. An eastward propagation speed is calculated from the bright feature between 0°, 5.5 UT and 10°, 5.75 UT in Figure 4b (endpoints indicated by the arrows marked 1a and 1b). At a range of 300 km from LNK, the distance span covered from 0° to 10° degrees is ~50 km and, along with the feature time span of 0.25 hours, gives a speed of ~55 m/s. Arrows 1–3 in Figure 3b (Δh fluctuations from LNK) indicate several features that have similar propagation speeds of ~55 m/s for times before ~5.75 UT. After that time, the features in both ΔR and Δh show a decreased speed of ~45 m/s, as indicated by the decreased slope of the features pointed out by arrows 4 and 5 in Figure 3b and by arrows 2 and 3 in Figure 4b. In the range-versus-time plots (Figures 3a and 4a), the negative slope of the features indicate that the fluctuations in both ionospheric height and reflection ratio are moving toward the LNK station from the storm. The eastward azimuthal and northward radial propagation measurements are shown schematically as arrows over the LNK shaded probed region in Figure 1.

[10] The azimuthal propagation speed measured by LBB for the feature between 123°, 5.5 UT and 110°, 5.70 UT in Figure 4d (marked by arrows 4a and 4b) is calculated to be ~85 m/s in the south-southeast direction (~25° from due south). The features in Figures 3d and 4d have similar slope throughout the entire 4-hour period, indicating that the propagation speed does not change much during that time. The radial propagation features detected by LBB (Figures 3c and 4c) have a negative slope, indicating that radial propagation is toward the LBB station from the storm. Propagation arrows are shown over the LBB probed region in Figure 1.

[11] From the LAM azimuthal plots (Figures 3f and 4f), clear propagation features (marked by arrows) with a speed of ~30 m/s in the northward direction are visible before ~5 UT, but after that there is no clear propagation in the azimuthal direction. The LAM radial measurement features have positive slope, indicating that they are moving eastward away from LAM toward the storm (Figures 3e and 4e). Arrows show the propagation directions over the shaded LAM probed region in Figure 1.

[12] Comparisons between perturbations in ionospheric height and peak reflection ratio (Figure 3 versus Figure 4) show similar periods and speeds for the fluctuations, but the fluctuations are not always in phase. This finding is consistent with the work of *Lay and Shao* [2011].

4. Discussion

[13] This study has made use of the technique described by *Lay and Shao* [2011] to probe fluctuations in apparent ionospheric height and peak reflection ratio in three regions near a large thunderstorm on the night of 17 June 2005. Measurements of the region directly north of the storm, probed by lightning detected at the LNK station, show propagation of the fluctuations in the eastward direction with a speed of ~55 m/s and in the northward direction away from the storm (Figure 1). The region to the southwest of the storm was probed by measurements at the LBB station and was found to have propagation in the west-southwest direction (away from the storm), as well as in the south-southeast direction with a speed of ~85 m/s (Figure 1). Measurements from the LAM station west of the storm show northward propagation of ~30 m/s before 5 UT and eastward propagation (toward the storm from the station) for the entire time period studied (Figure 1).

[14] The northward propagation measured at LNK and the southward propagation measured at LBB strongly indicate that the fluctuations are moving away from the thunderstorm. The eastward propagation measured at all three LASA stations suggests a background eastward atmospheric gravity wave that is perturbing the D-layer electron density. Because the LAM station is 'upwind' from the thunderstorm, the background AGW dominates the behavior of the ionosphere at that location.

[15] The northward propagating features measured at the LAM station before 5 UT (Figures 3f and 4f) could be fluctuations driven by the small storm near the LBB station shown in Figure 1. The small storm cell is about 200 km directly south of the center of the ionospheric region probed by LAM shown in the shaded oval in Figure 1. Given the measured propagation speed of 30 m/s (Figures 3f and 4f),

the fluctuation would take slightly less than 2 hours to reach the center of the region probed by the LAM station. Figure 1 shows that the cell was convectively active from ~0 UT to 3 UT; timing that is consistent with a 2-hour delay in the measured perturbations 200 km away.

[16] These multi-station measurements provide further support for propagating ionospheric disturbances produced in the thunderstorm region. Furthermore, the Oklahoma Lightning Mapping Array (OK-LMA) measured significant lightning activity above the tropopause between 2 and 3 UT within 150 km of the center of the OK-LMA (M. Elliott, personal communication, 2011). These signatures above the tropopause provide further support to the hypothesis that several of the observed perturbations presented in this paper are caused by atmospheric gravity waves (AGWs) that are originated from convective thunderstorm activity overshooting the tropopause. In addition to ionospheric perturbations generated by thunderstorms, these results also show variability in the D-layer due to larger-scale background AGWs, indicating that it is likely that the D-layer ionospheric profile is rarely static. Determining the magnitude of variability in the typical exponential profile height and steepness variability is currently in progress.

[17] **Acknowledgements.** This research was supported by the Los Alamos National Laboratory's Laboratory Directed Research and Development (LDRD) project 20110184ER.

[18] The Editor thanks Robert Moore and an anonymous reviewer for their assistance in evaluating this paper.

References

Alexander, M. J., J. R. Holton, and D. R. Durran (1995), The gravity wave response above deep convection in a squall line simulation, *J. Atmos. Sci.*, *52*, 2212–2226, doi:10.1175/1520-0469(1995)052<2212:TGWRAD>2.0.CO;2.

Bickel, J. E., J. A. Ferguson, and G. V. Stanley (1970), Experimental observation of magnetic field effects on VLF propagation at night, *Radio Sci.*, *5*, 19–25, doi:10.1029/RS005i001p00019.

Cheng, Z., S. A. Cummer, H.-T. Su, and R.-R. Hsu (2007), Broadband very low frequency measurement of D region ionospheric perturbations caused by lightning electromagnetic pulses, *J. Geophys. Res.*, *112*, A06318, doi:10.1029/2006JA011840.

Cummer, S. A., U. S. Inan, and T. F. Bell (1998), Ionospheric D region remote sensing using VLF radio atmospherics, *Radio Sci.*, *33*, 1781–1792, doi:10.1029/98RS02381.

Han, F., and S. A. Cummer (2010), Midlatitude daytime D region ionosphere variations measured from radio atmospherics, *J. Geophys. Res.*, *115*, A10314, doi:10.1029/2010JA015715.

Inan, U. S., V. P. Pasko, and T. F. Bell (1996), Sustained heating of the ionosphere above thunderstorms as evidenced in the early/fast VLF events, *Geophys. Res. Lett.*, *23*, 1067–1070, doi:10.1029/96GL01360.

Jacobson, A. R., X.-M. Shao, and R. Holzworth (2009), Full-wave reflection of lightning long-wave radio pulses from the ionospheric *D* region: Numerical model, *J. Geophys. Res.*, *114*, A03303, doi:10.1029/2008JA013642.

Lay, E. H., and X.-M. Shao (2011), High temporal and spatial-resolution detection of D-layer fluctuations by using time-domain lightning waveforms, *J. Geophys. Res.*, *116*, A01317, doi:10.1029/2010JA016018.

McRae, W. M., and N. R. Thomson (2000), VLF phase and amplitude: Daytime ionospheric parameters, *J. Atmos. Sol. Terr. Phys.*, *62*, 609–618, doi:10.1016/S1364-6826(00)00027-4.

Pappert, R. A., and J. A. Ferguson (1986), VLF/LF mode conversion model calculations for air to air transmissions in the Earth-ionosphere waveguide, *Radio Sci.*, *21*, 551–558, doi:10.1029/RS021i004p00551.

Pasko, V. P., U. S. Inan, Y. N. Taranenko, and T. F. Bell (1995), Heating, ionization and upward discharges in the mesosphere due to intense quasi-electrostatic thundercloud fields, *Geophys. Res. Lett.*, *22*, 365–368, doi:10.1029/95GL00008.

Shao, X.-M., and A. R. Jacobson (2009), Model simulation of very low frequency and low frequency lightning signal propagation over intermediate ranges, *IEEE Trans. Electromagn. Compat.*, *51*, 519–525, doi:10.1109/TEMC.2009.2022171.

Shao, X.-M., M. Stanley, A. Regan, J. Harlin, M. Pongratz, and M. Stock (2006), Total lightning observations with the new and improved Los Alamos Sferic Array (LASA), *J. Atmos. Oceanic Technol.*, *23*, 1273–1288, doi:10.1175/JTECH1908.1.

Thomson, N. R., C. J. Rodger, and M. A. Clilverd (2005), Large solar flares and their ionospheric D region enhancements, *J. Geophys. Res.*, *110*, A06306, doi:10.1029/2005JA011008.

Vadas, S. L., and D. C. Fritts (2004), Thermospheric responses to gravity waves arising from mesoscale convective complexes, *J. Atmos. Sol. Terr. Phys.*, *66*, 781–804, doi:10.1016/j.jastp.2004.01.025.

Vadas, S. L., J. Yue, C.-Y. She, P. A. Stamus, and A. Z. Liu (2009), A model study of the effects of winds on concentric rings of gravity waves from a convective plume near Fort Collins on 11 May 2004, *J. Geophys. Res.*, *114*, D06103, doi:10.1029/2008JD010753.

Wait, J. R., and K. P. Spies (1964), *Characteristics of Earth-Ionosphere Waveguide for VLF Radio Waves*, Natl. Bur. Stand., Boulder, Colo.

Yue, J., S. L. Vadas, C.-Y. She, T. Nakamura, S. C. Reising, H.-L. Liu, P. Stamus, D. A. Krueger, W. Lyons, and T. Li (2009), Concentric gravity waves in the mesosphere generated by deep convective plumes in the lower atmosphere near Fort Collins, Colorado, *J. Geophys. Res.*, *114*, D06104, doi:10.1029/2008JD011244.

E. H. Lay and X.-M. Shao, Space and Remote Sensing Group, Los Alamos National Laboratory, MS D436, Los Alamos, NM 87545, USA. (elay@lanl.gov; xshao@lanl.gov)